ARMY RESEARCH LABORATORY

Superresolution for Low-Cost Enabling Radar Technology

Canh Ly and Herbert Dropkin

ARL-TR-1780 October 1998

The findings in this report are not to be construed as an official Department of the Army position unless so designated by other authorized documents.

Citation of manufacturer's or trade names does not constitute an official endorsement or approval of the use thereof.

Destroy this report when it is no longer needed. Do not return it to the originator.

Army Research Laboratory

Adelphi, MD 20783-1197

ARL-TR-1780 **October 1998**

Superresolution for Low-Cost Enabling Radar Technology

Canh Ly and Herbert Dropkin

Sensors and Electron Devices Directorate

Abstract

The MUltiple SIgnal Classification (MUSIC) algorithm has been used widely in applications with spatially distributed sensor arrays. In these applications, the algorithm uses the phase relations of the signal at different sensor pointing angles. Accordingly, the MUSIC algorithm has not been used by others to superresolve target positions within the main beam of a radar with a single narrow-beam antenna that is step-scanned in angle because there is no phase shift due to the scanning of the beam. We have developed an application called Scan MUSIC (SMUSIC) for the spatial resolution of closely spaced targets with a stepped-scan radar. We apply SMUSIC to resolve closely spaced coherent targets when a one-dimensional stepped scanning antenna is used. As the low-cost enabling radar technology (LCERT) antenna points at different angles in the horizontal (azimuth) direction, a step-scan sensor vector is formed. In this report, we demonstrate that SMUSIC can be used for a scanning antenna using experimental LCERT radar data. We also show the problems encountered when using experimental data from targets exhibiting constructive and destructive interferences.

Contents

Appendices

Figures

Tables

1. Introduction

The Rayleigh criterion limits the angular resolution of an antenna aperture of size D to the value $\theta = \lambda/D$, where λ is the wavelength corresponding to the transmitted frequency. The MUltiple SIgnal Classification (MUSIC) algorithm [1], which uses the eigenvector decomposition method, is a superresolution algorithm widely used to locate closely spaced multiple emitters (targets) with high resolution (smaller than the Rayleigh criterion). The algorithm is often employed with a uniform linear array of sensors of total aperture length D and depends on the phase progression between sensors of the returned signal. In contrast, a single antenna, also of aperture D and having a beamwidth θ, which is scanned in angle, generates no phase shifts within the main lobe due to the target direction. Therefore, the MUSIC algorithm has not been used by others to superresolve target positions within the main beam of a single narrow-beam antenna. In this report, we describe an application called Scan MUSIC (SMUSIC) [2] that is used to improve the spatial resolution of closely spaced targets with a stepped-scan radar. The signal amplitude vector formed by the response of the antenna as it is stepped in angle replaces the vector of multiple sensor outputs of a uniformly linear spaced array of sensors. In many cases, this replacement of a large number of sensors by a single rotatable sensor may be advantageous. We demonstrate that superresolution is obtainable in this stepped-scan case, albeit with the requirement for a higher signal-to-noise ratio (SNR) than that required for an antenna array of spaced elements having the same Rayleigh resolution. We show results of SMUSIC using the data obtained with an experimental system called the low-cost enabling radar technology (LCERT) radar [3] as the radar antenna scanned horizontally in the region of interest (ROI).

2. LCERT Experimental Data

The LCERT instrumentation radar system operates at Ku-band (16 GHz) and is placed on a truck trailer platform. The antenna was mounted on a pedestal and had a relatively wide elevation beam (cosecant-squared antenna) and a narrow azimuth beamwidth (less than 1.5°). The radar has two operating modes (stationary target indicator (STI) and moving target indicator (MTI)) and different modulation modes (linear frequency modulation (LFM) and phase modulation (PM)). It is computer-controlled with a high data rate recording capability. Table 1 shows the characteristics of LCERT radar.

The experimental data for this SMUSIC analysis were collected at an Aberdeen Proving Ground (APG), MD, test range in 1997. The test range is a flat, grassy, and open field. The coherent returned signals were collected as the LCERT antenna scanned horizontally in the ROI, which had corner reflectors (targets) within the main beam of the antenna. Figure 1 shows the antenna used in the data collection.

The antenna amplitude pattern was obtained using an aluminum trihedral (corner reflector or target) with radar cross section (RCS) = 21.5 dBsm as a single target. This was placed 600 m downrange at the center of the radar line-of-sight axis. The antenna amplitude data were used as the array manifold vector for the SMUSIC algorithm.

Two other aluminum targets (shown in fig. 2), with RCS = 17.0 dBsm, were placed at a cross-range position 600 m downrange from the radar. All corner reflectors faced the radar. The antenna continuously scanned within ±3° of the ROI with respect to the center of the antenna axis (0°) (see fig. 3). The targets were set up in cross range as shown in figure 4. The experimental scan data were obtained by strobing the sampling data from the slowly scanning antenna.

Table 1. LCERT radar characteristics.

Parameter	Value
Transmit frequency (GHz)	16
Transmit pulsewidth (μs)	2.48
Receive pulsewidth (μs)	5.12
Transmit chirp rate (MHz/μs)	8.065
Transmit start frequency (MHz)	100
Receive start frequency (MHz)	99.625
Pulse repetition frequency (kHz)	8
Analog-to-digital samples per pulse	256
Pulses per coherent processing interval	32
Range resolution (m)	10.8
Number of coherent processing intervals	1000
Radar mode (STI or MTI)	STI
Modulation (1-LFM, 2-PM)	1
Azimuth angular scan swath (°)	8
Scan rate (°/s)	4

Figure 1. LCERT antenna.

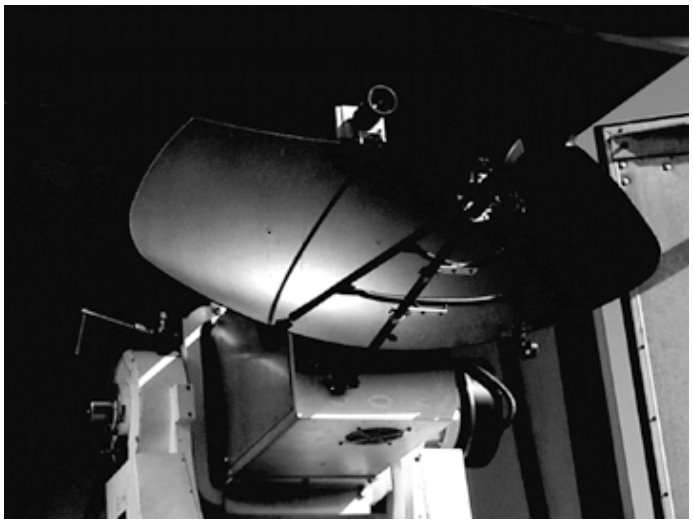

Figure 2. Corner reflectors for experimental setup.

Figure 3. LCERT experimental setup.

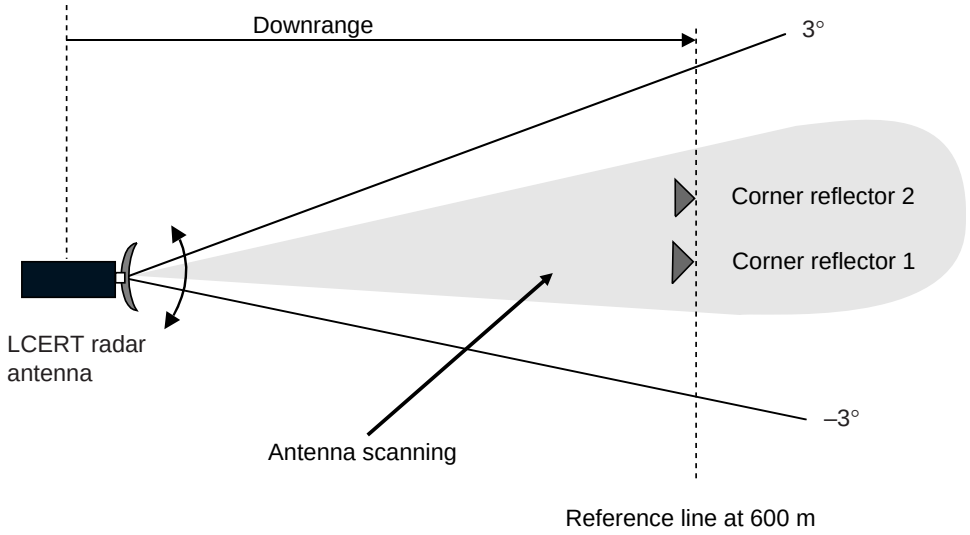

Figure 4. Target placement for LCERT experimental setup.

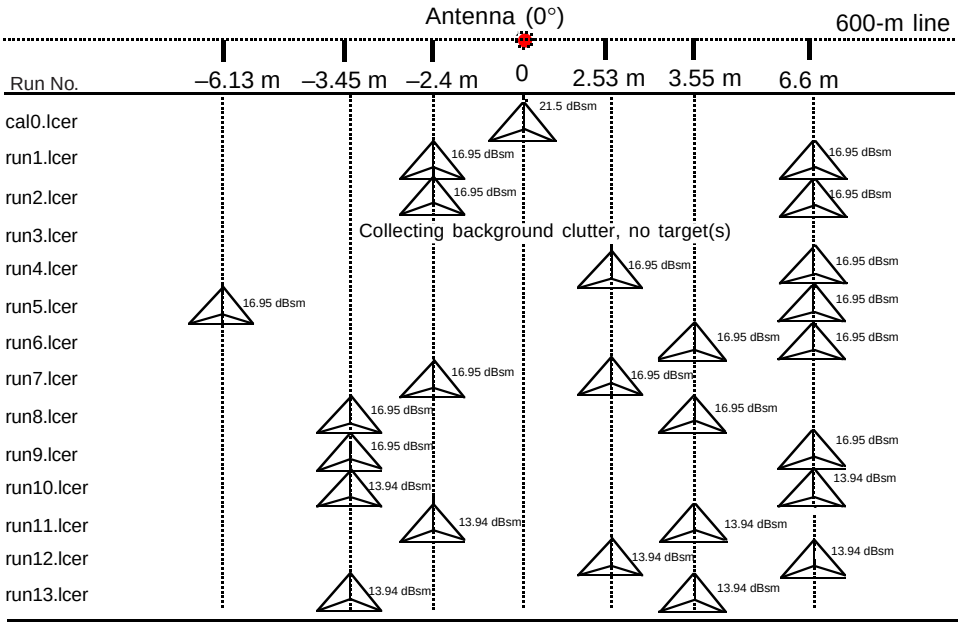

In figure 4, the vertical dotted lines are the actual corner reflector positions at 600 m downrange. All corner reflectors (targets) are within the main lobe of the antenna beam since the cross range is about 13.6 m for the antenna beamwidth 1.3°. All the runs except the first run, cal0.lcer, and run 3 had two targets placed as shown in the figure and covered as many combinations for $\frac{1}{2}$, $\frac{1}{3}$, $\frac{1}{4}$, $\frac{3}{4}$ beamwidth of the antenna. For runs 10 to 13, we used two smaller RCS targets (13.94 dBsm) to determine whether SMUSIC can resolve closely spaced targets at lower RCS.

The radar was externally calibrated every time data were collected by using the standard method of checking the maximum return of a single corner reflector mounted on a tripod.

The LCERT radar data were first preprocessed by the direct sampling method [4,3] to obtain the I (in-phase) and Q (quadrature or out-of-phase) components as well as the magnitude of the data, which are suitable formats for the SMUSIC algorithm. Figure 5 shows the layout of the raw data stored in a data file.

The data contained 1000 coherent processing intervals (CPIs). Each CPI consisted of 32 pulses (0, 1, … , 31), and 256 samples for each pulse. Within each CPI, the frequency was chirped (linear frequency modulated)

Figure 5. Raw data format.

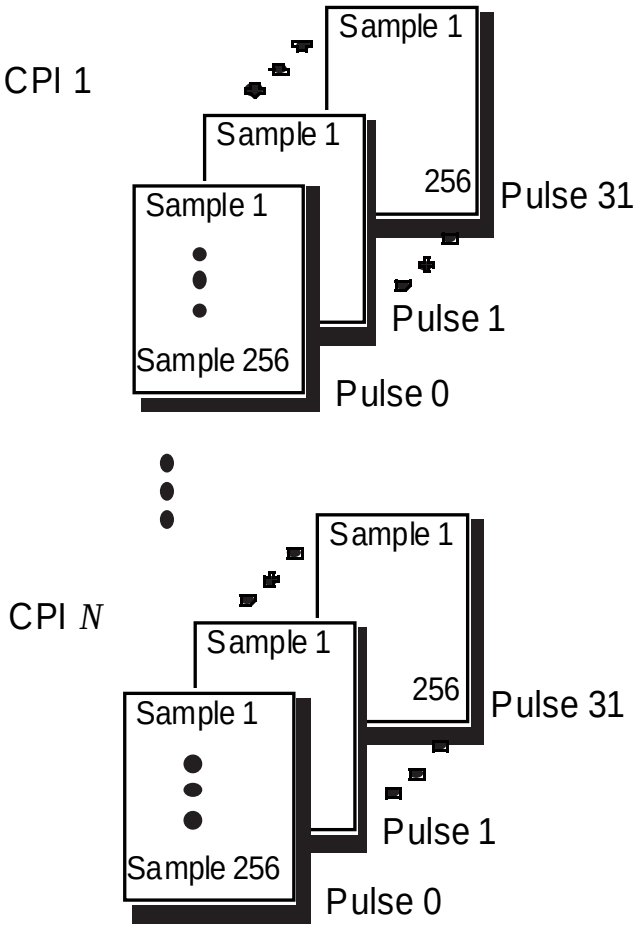

with a bandwidth of 20 MHz for each pulse, and the starting frequencies for the pulses were set at increments of 20 MHz so that the total bandwidth was 640 MHz. Then the first 550 CPI were used and pulse 0 was selected for each CPI to apply the SMUSIC algorithm (other pulses give the same results). Figure 6 is a block diagram of the preprocessed LCERT data before the SMUSIC process.

In figure 7, data from the first run, cal0.lcer, show the antenna pattern obtained when the LCERT radar antenna scanned within ±3° of the ROI for a single reflector. Figures 8 and 9 are examples of the responses that exhibit two types of interference from constructive and destructive interference. Figure 8 shows the target response of two reflectors within the main lobe of the antenna that constructively interfere. Figure 9 shows the target response of the same two reflectors when they destructively interfere.

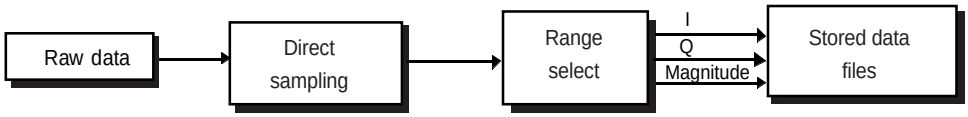

Figure 6. Block diagram of preprocessing of LCERT raw data.

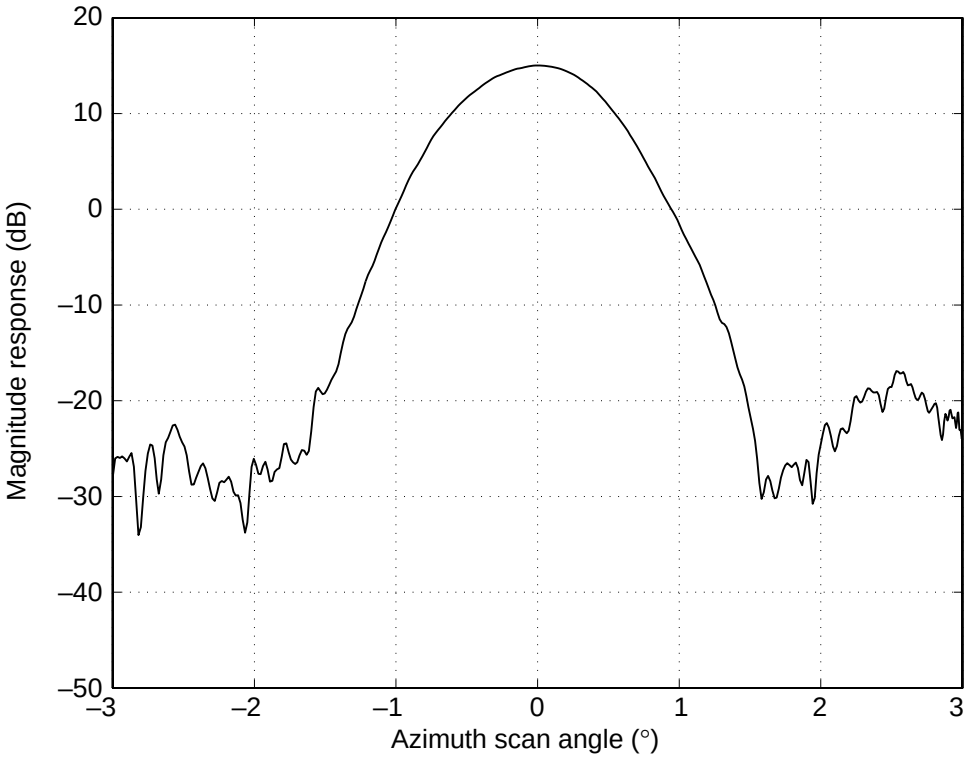

Figure 7. LCERT antenna pattern.

Figure 8. Constructive target response.

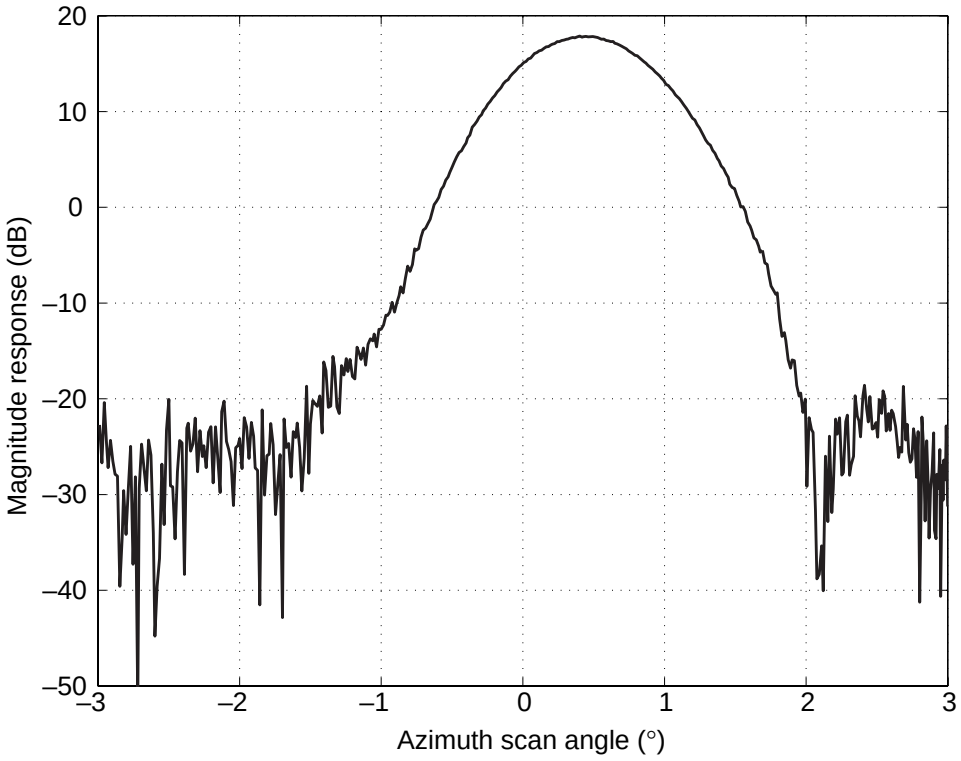

Figure 9. Destructive target response.

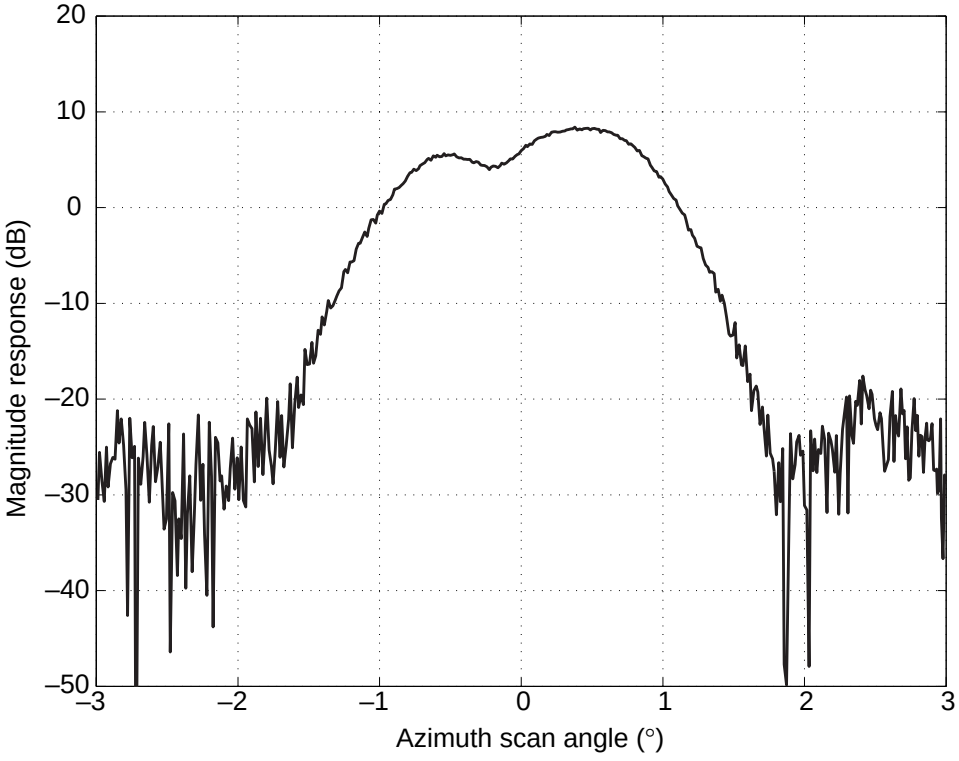

3. SMUSIC Process

Figure 10 depicts the processing sequence of the SMUSIC algorithm. In this figure, the LCERT block provides the LCERT data collected at APG. The data samples are the data centered with respect to the center of the antenna pattern. The data were then truncated between ±3°; these are called truncated data. Finally, the data samples were taken from every 6th sample of the truncated data between ±1.5° to be used for the SMUSIC computation. These steps were done in the PRE-format block.

In general, we can write the correlation matrix of a complex random vector, $\mathbf{x}$, as $\mathbf{R} = e[\mathbf{x}\mathbf{x}^H]$, where $\mathbf{x}$ is the vector of observed data and is referred to as a snapshot, and the elements of a snapshot are called samples. $e[\ ]$ is the expected value or ensemble average operator, and H is Hermitian transpose. Then the data vector, $\mathbf{x}$, with N samples, was used to estimate the correlation matrix. Since there is only a single snapshot (scan) and the target response is coherent, $\hat{\mathbf{R}}_{\mathbf{xx}}$ will be rank deficient. In fact, the rank of $\hat{\mathbf{R}}_{\mathbf{xx}}$ is equal to 1 (a proof of this property is given by Shan et al [5]). The following simple example demonstrates this problem.

Let a vector $\mathbf{x} = [1\ 3\ 5\ 7\ 4]^T$. Then

$$\hat{\mathbf{R}}_{\mathbf{xx}} = \begin{bmatrix} 1 & 3 & 5 & 7 & 4 \\ 3 & 9 & 15 & 21 & 12 \\ 5 & 15 & 25 & 35 & 20 \\ 7 & 21 & 35 & 49 & 28 \\ 4 & 12 & 20 & 28 & 16 \end{bmatrix}.$$

Then the rank of $\hat{\mathbf{R}}_{\mathbf{xx}}$ is equal to 1 because the columns of $\hat{\mathbf{R}}_{\mathbf{xx}}$ are linearly dependent. To avoid the rank deficient problem, Evans [6] developed a technique called forward/backward spatial smoothing. For more information and a further explanation of this technique, see Van Trees [7]. In this application, we only use forward spatial smoothing to obtain the full rank of $\hat{\mathbf{R}}_{\mathbf{xx}}$ and also decorrelate the coherent signals. We call this the forward subvector averaging technique and use it to estimate the correlation matrix as described below. The nonsingularity of the sample correlation matrix, $\hat{\mathbf{R}}_{\mathbf{xx}}$, is crucial to an application of the eigenvector decomposition method; the technique guarantees the nonsingularity of the sample correlation matrix of the signals.

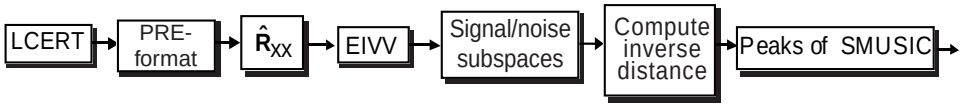

Figure 10. Block diagram of SMUSIC process.

Let $\mathbf{x}$ be an $N \times 1$ input data vector. Define subvectors $\mathbf{x}^{(i)}$ for $1 < i < p$ (number of subvectors), to be a vector containing Q consecutive samples from $\mathbf{x}$ with $Q < N$, starting at sample i as shown in equation (1):

$$\begin{aligned} \mathbf{x}^{(1)} &= \left[\mathbf{x}_1, \mathbf{x}_2, \cdots, \mathbf{x}_Q\right]^T , \\ \mathbf{x}^{(2)} &= \left[\mathbf{x}_2, \mathbf{x}_3, \cdots, \mathbf{x}_{Q+1}\right]^T , \\ &\vdots \\ \mathbf{x}^{(p)} &= \left[\mathbf{x}_p, \mathbf{x}_{p+1}, \cdots, \mathbf{x}_{p+Q-1}\right]^T . \end{aligned} \tag{1}$$

Since there are N samples in $\mathbf{x}$, the possible values of p and Q are related to N by

$$p + Q - 1 = N . \tag{2}$$

Next, let the subvector correlation matrix $\hat{\mathbf{R}}^{(i)}$ be of $\mathbf{x}^{(i)}\,\mathbf{x}^{(i)H}$. Finally, define the estimate correlation matrix $\hat{\mathbf{R}}_{\mathbf{xx}}$ to be the average of p subvector correlation matrices as

$$\hat{\mathbf{R}}_{\mathbf{xx}} = \frac{1}{p}\sum_{i=1}^{p} \hat{\mathbf{R}}^{(i)} = \frac{1}{p}\sum_{i=1}^{p} \mathbf{x}^{(i)}\,\mathbf{x}^{(i)H} , \tag{3}$$

computed in the $\hat{\mathbf{R}}_{\mathbf{xx}}$ block. Note that the matrices $\hat{\mathbf{R}}^{(i)}$ and $\hat{\mathbf{R}}_{\mathbf{xx}}$ are of the order of $Q \times Q$, while $\mathbf{R}$ is of the order of $N \times N$. So, by the subvector averaging technique, the dimension of the sample correlation matrix is effectively reduced. The following example demonstrates this technique.

Let $\mathbf{x}$ be the input data vector as used above, let $p = 3$, so $Q = 3$; then

$$\mathbf{x}^{(1)} = [1\ 3\ 5]^T , \mathbf{x}^{(2)} = [3\ 5\ 7]^T , \text{ and } \mathbf{x}^{(3)} = [5\ 7\ 4]^T .$$

Then $\hat{\mathbf{R}}_{\mathbf{xx}}$ is computed using equation (3) as

$$\hat{\mathbf{R}}_{\mathbf{xx}} = \begin{bmatrix} 11.6667 & 17.6667 & 15.3333 \\ 17.6667 & 27.6667 & 26.0000 \\ 15.3333 & 26.0000 & 30.0000 \end{bmatrix} ,$$

and the rank of $\hat{\mathbf{R}}_{\mathbf{xx}}$ is 3, which is full rank. We see that the original correlation matrix has the dimension 5×5, and the estimate correlation matrix using the subvector averaging technique has the dimension 3×3. The trade-off with this technique clearly shows that the dimension is effectively reduced but the rank is increased.

If the estimated correlation matrix is nonsingular, the distinct eigenvalues and corresponding eigenvector space from the estimate $\hat{\mathbf{R}}_{\mathbf{xx}}$ are

$$\{\lambda_1 \geq \lambda_2, \ldots, \geq \lambda_Q\} \text{ and } \{v_1, v_2, \ldots v_Q\} . \quad (4)$$

The computation is carried in the EIVV (eigenvectors and eigenvalues) block (see fig. 10).

From the argument above, if there are M targets, the rank of $\hat{\mathbf{R}}_{\mathbf{xx}}$ will be M. It follows that the minimal eigenvalues of $\hat{\mathbf{R}}_{\mathbf{xx}}$ are $\{\lambda_{M+1} \geq \lambda_{M+2}, \ldots, \geq \lambda_Q\}$, and the eigenvectors corresponding to the minimal eigenvalues are $\{v_{M+1}, v_{M+2}, \ldots, v_Q\}$. These eigenvectors span the noise subspace. The orthogonal complement of the noise subspace is referred to as the signal subspace. The signal subspace denotes $\hat{\mathbf{U}}_{\mathbf{S}}$, and the noise subspace denotes $\hat{\mathbf{U}}_{\mathbf{N}}$. The dimension of $\hat{\mathbf{U}}_{\mathbf{S}}$ is $Q \times M$ and $\hat{\mathbf{U}}_{\mathbf{N}}$ is $Q \times (Q - M)$. In this experiment, since we know the number of targets in the field, $M = 2$, we use this information to separate the eigenvector space into a signal eigenvector with dimension $Q \times 2$ and noise eigenvector with dimension $Q \times (Q - 2)$ subspaces in the Signal/noise subspaces block.

We compute the SMUSIC spectrum using equation (5) in the Compute inverse distance block. The SMUSIC algorithm uses the orthogonality property that exists between the signal eigenvector subspace and the noise eigenvector subspace from the sample correlation matrix to estimate the position of each target center. This can be accomplished by computing the inverse of the distance of a searching or true direction or an array manifold vector at angle θ and the noise eigenvector subspace. The peaks, computed in the Peaks of SMUSIC block, from the SMUSIC spectrum are the estimated target locations

$$P_{MU}(\theta) = \left(v(\theta)^H \hat{\mathbf{U}}_{\mathbf{N}} \hat{\mathbf{U}}_{\mathbf{N}}{}^H v(\theta) \right)^{-1} , \quad (5)$$

where $v(\theta)$, that is, the scanning antenna pattern, is the steering vector or array manifold vector for all values of θ.

In the SMUSIC computation, we used the LCERT antenna pattern as the array manifold vector to compute the spectral SMUSIC. The array manifold vector for this scanning antenna in this report is a magnitude two-way scanning antenna pattern. Unlike the ordinary MUSIC, which mostly uses a uniformly linear array manifold vector for the computation, the steering vector of the SMUSIC does not depend on the phase relationship from one step scan to another step scan.

4. Results

In this section, we show the LCERT experimental data collected at APG in section 4.1 and the results of SMUSIC in section 4.2.

4.1 LCERT Data

The magnitudes of the target responses in decibels versus azimuth scan angle in degrees for all runs are shown in figures A-1 to A-13 in appendix A. Figure A-1 is the LCERT antenna pattern used as the array manifold vector for the SMUSIC computation. From this figure, we see that the noise from the response, including the system noise and the background noise, is small compared to the signal response. From figures A-2 to A-13, we see that the responses exhibit varying types of interferences from constructive to partially constructive to destructive interferences. Figures A-2, A-4, A-6, A-8, and A-13 show the target responses of two reflectors within the main lobe of the antenna that constructively interfere. Figures A-3, A-5, A-7, and A-9 to A-12 show the targets responses of the same two reflectors when they fully and partially destructively interfere. These types of interferences affect the performance of SMUSIC.

4.2 SMUSIC Results

LCERT data included two different cases: constructive and destructive interferences. For the constructive interference, SMUSIC resolved the closely spaced targets when the targets were placed apart at distances less than the beamwidth of the antenna. On the other hand, for the destructive interference, SMUSIC was not able to resolve the closely spaced targets within the beamwidth of the antenna. In attempts to resolve targets having destructive interference, we use the phase information of the data as well as the phase information of the manifold vector. We used complex arithmetic for the SMUSIC process. However, SMUSIC was still unable to resolve the targets.

Figures B-1 to B-12 in appendix B show the results of SMUSIC for LCERT data runs. In this SMUSIC application, we only used the magnitude information of the scanning antenna and the target response for superresolving the targets within the main lobe of the antenna beam.

5. Conclusions and Future Investigations

We have demonstrated that a superresolution algorithm like MUSIC can be extended for a scanning antenna even though there is ideally no phase variation for the scanning antenna within the main beam of an antenna. We have developed an application called SMUSIC to apply to the scanning antenna that used the magnitude of the target response to superresolve two closely spaced targets within the main beam of the LCERT radar antenna. SMUSIC resolved the closely spaced targets when they interfered constructively; i.e., they were within 30° or less phase shift of each other.

We showed the results of SMUSIC for all the cases of partially or fully constructive interference. We conclude that SMUSIC can be used for real data with a narrow-band signal and that it performs beyond the limit of the Rayleigh criterion. It can resolve the target locations in which the target separation is less than one-third of an antenna beamwidth.

For the fully and partially destructive interference cases, SMUSIC may not be able to resolve the targets within the antenna beamwidth. This problem needs further investigation.

An advantage of a scanning antenna is that it avoids the requirement of a phase calibration of a linear array of sensors. A single sensor can be cheaper than making multiple sensors with the same aperture length.

A more comprehensive Monte Carlo study is needed to analyze the performance of the SMUSIC algorithm for a scanning antenna in terms of the antenna beamwidth, mean-square-error (MSE), probability of successful resolution (PSR) in a function of the number of step scans, numbers of subvector averaging, and SNR for two coherent targets with different degrees of correlation.

Acknowledgments

The authors thank Eric Adler, John Clark, Marvin Conn, Phuong Phu, and Barry Scheiner for their corporation in collecting experimental data. The authors also thank Joseph Nemarich and Brian Sadler for many helpful comments and discussions.

References

1. Ralph O. Schmidt, "Multiple Emitter Location and Signal Parameter Estimation," *IEEE Trans. on Ant. and Prop.*, 34(3) (March 1986), pp 276–280.
2. Herbert Dropkin and Canh Ly, "Superresolution for Scanning Antenna," *Proc. of the 1997 IEEE National Radar Conf.* (May 1997), pp 306–308.
3. Eric Adler, John Clark, Marvin Conn, Phuong Phu, and Barry Scheiner, "Low-Cost Enabling Technology for Multimode Radar Requirements," *Proc. of the 1998 IEEE Radar Conf.* (May 1998).
4. Barry Scheiner, *Signal Processing for a Low-Cost Multimode Radar*, forthcoming report.
5. Tie-Jun Shan, Mati Wax, and Thomas Kailath, "On Spatial Smoothing for Direction-of-Arrival Estimation of Coherent Signals," *IEEE Trans. on Acoustics, Speech, and Sig. Proc.*, ASSP-**33**, 4 (August 1985), pp 806–811.
6. J. E. Evans, J. R. Johnson, and D. F. Sun, *Application of Advanced Signal Processing Techniques to Angle of Arrival Estimation in ATC Navigation and Surveillance*, technical report 582, Lincoln Laboratory, Massachusetts Institute of Technology, Lexington, MA (June 1982).
7. Harry L. Van Trees, "Class Notes: INFT934: Array Processing: Detection and Estimation Theory, Vol. IV," George Mason University, Fairfax, VA (January 1997).

Appendix A. LCERT Magnitude Response

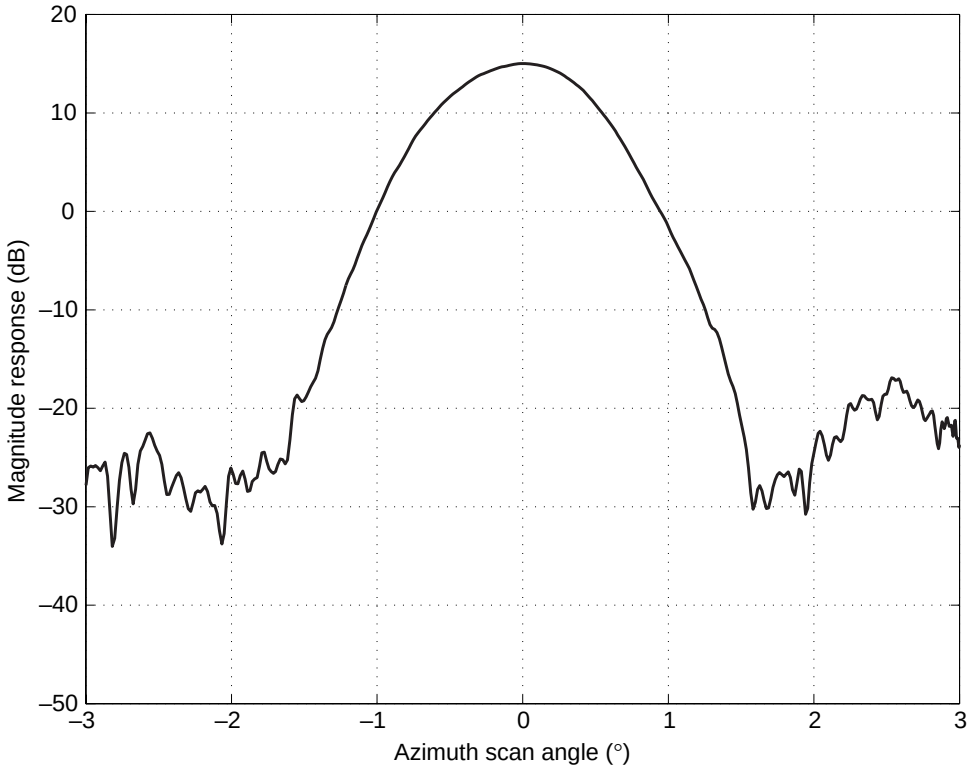

Figure A-1. LCERT antenna pattern (skip data point (SDP) = 6).

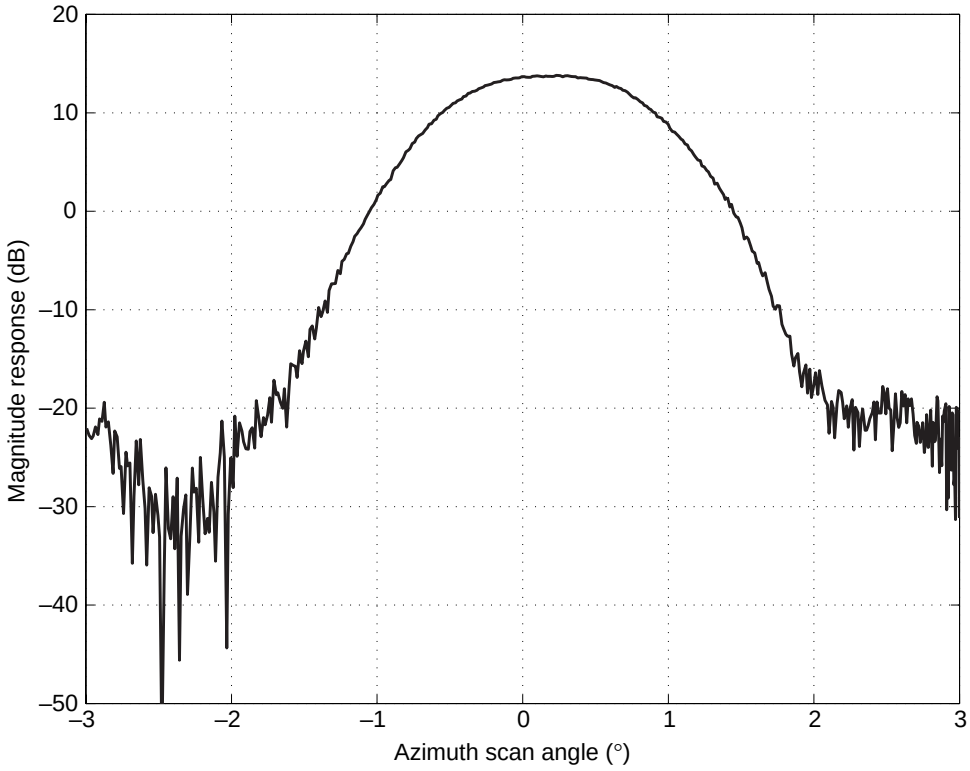

Figure A-2. LCERT data run 1 (SDP = 6).

Figure A-3. LCERT data run 2 (SDP = 6).

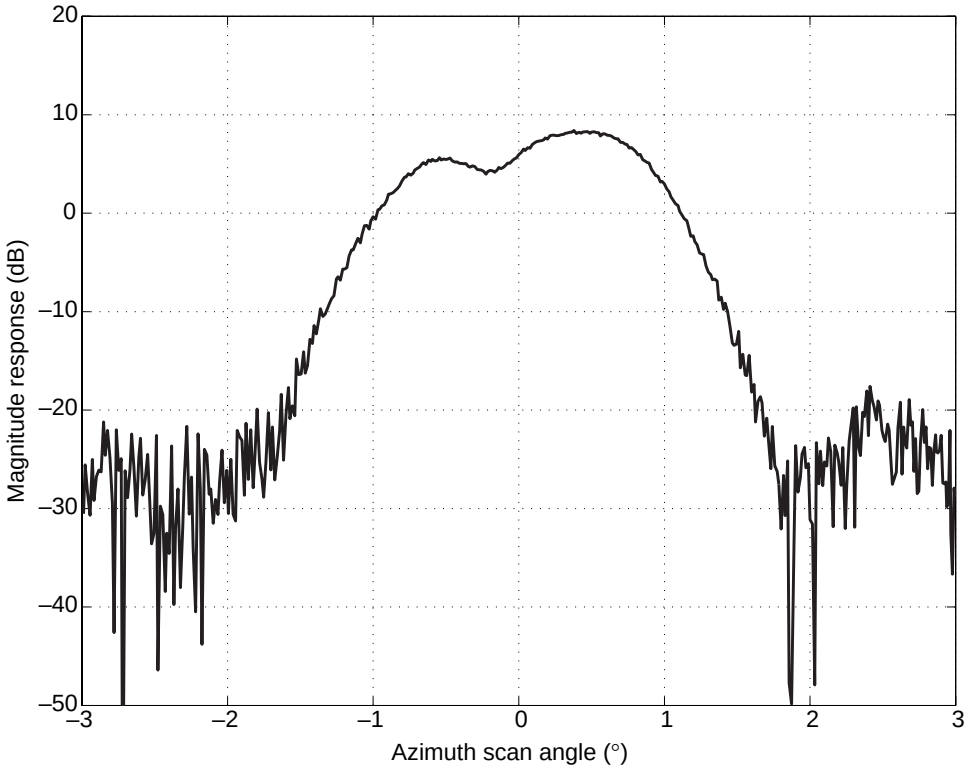

Figure A-4. LCERT data run 4 (SDP = 6).

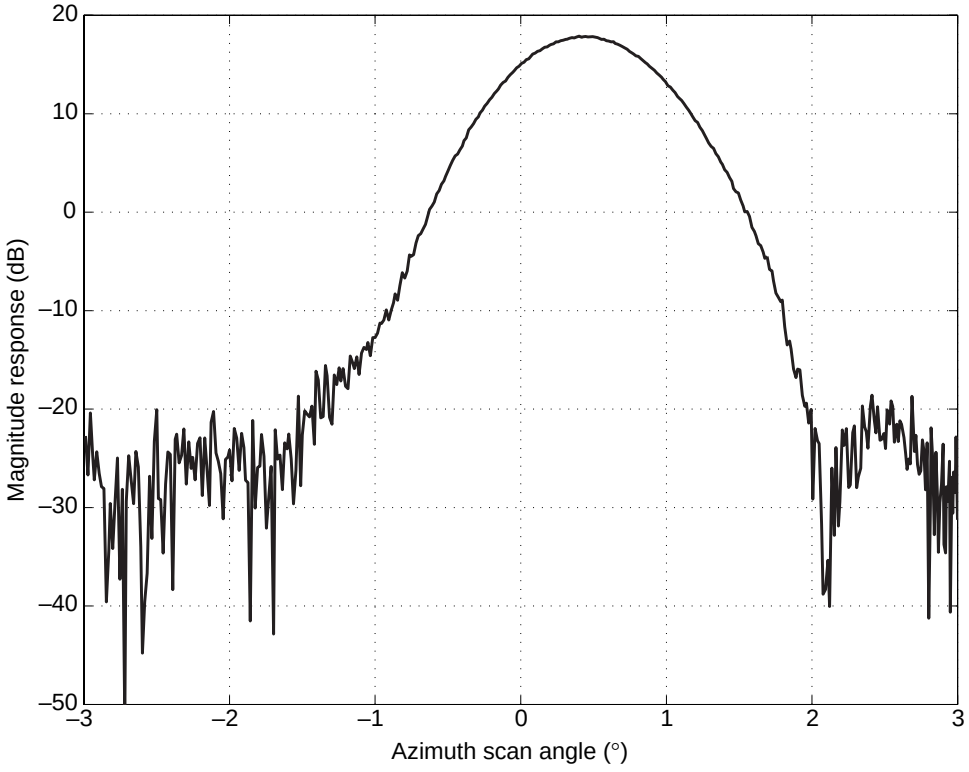

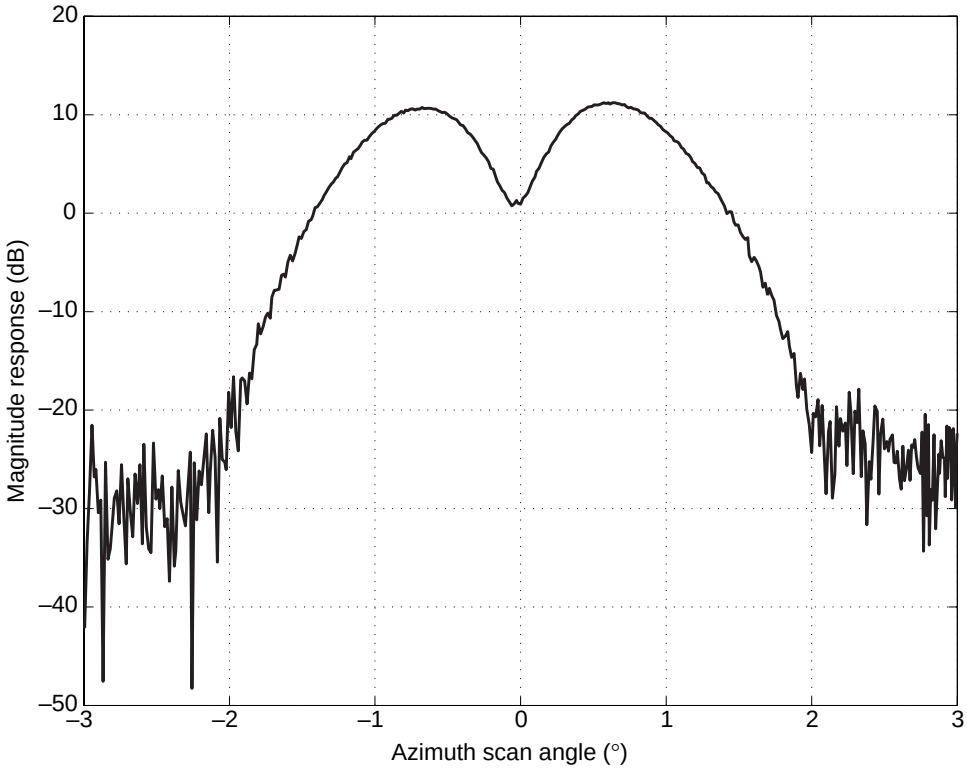

Figure A-5. LCERT data run 5 (SDP = 6).

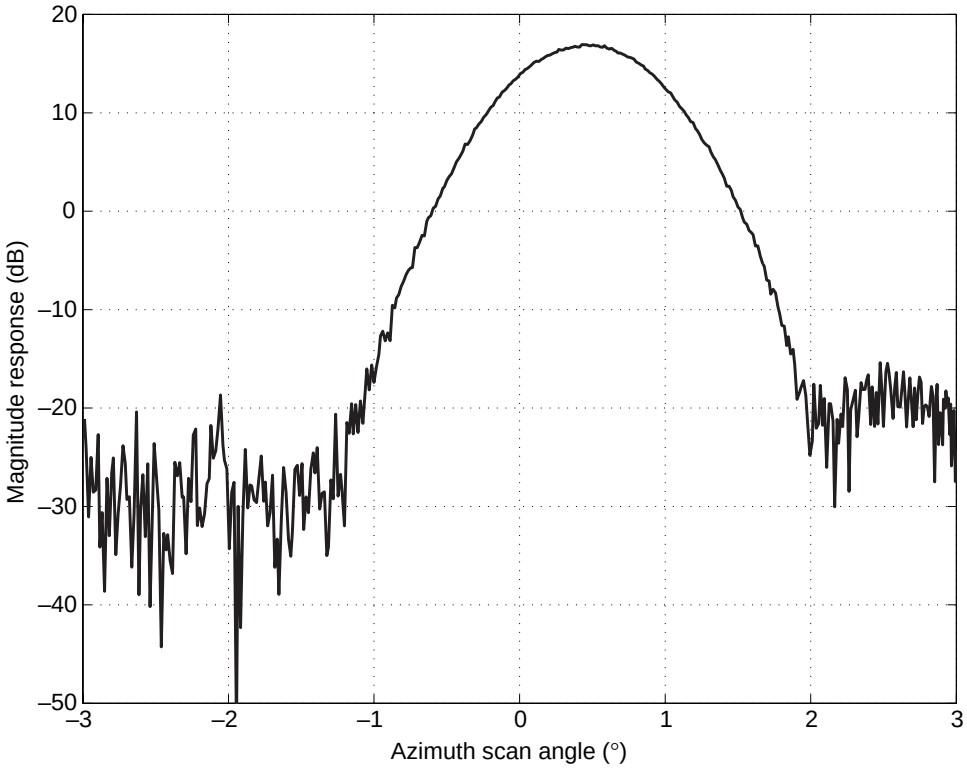

Figure A-6. LCERT data run 6 (SDP = 6).

Figure A-7. LCERT data run 7 (SDP = 6).

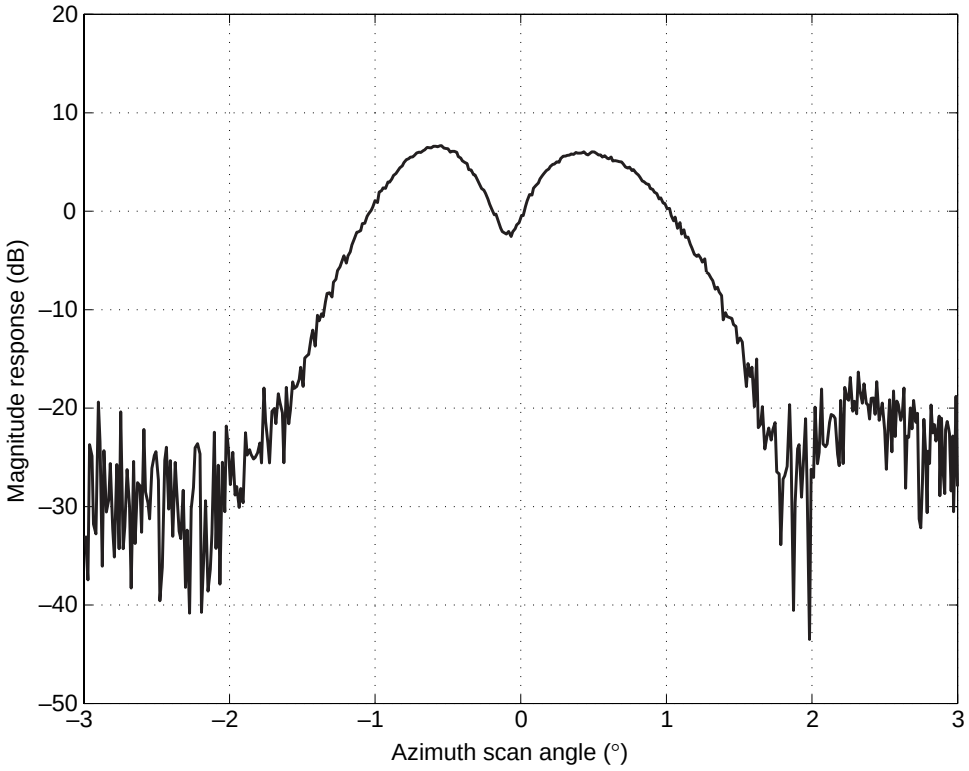

Figure A-8. LCERT data run 8 (SDP = 6).

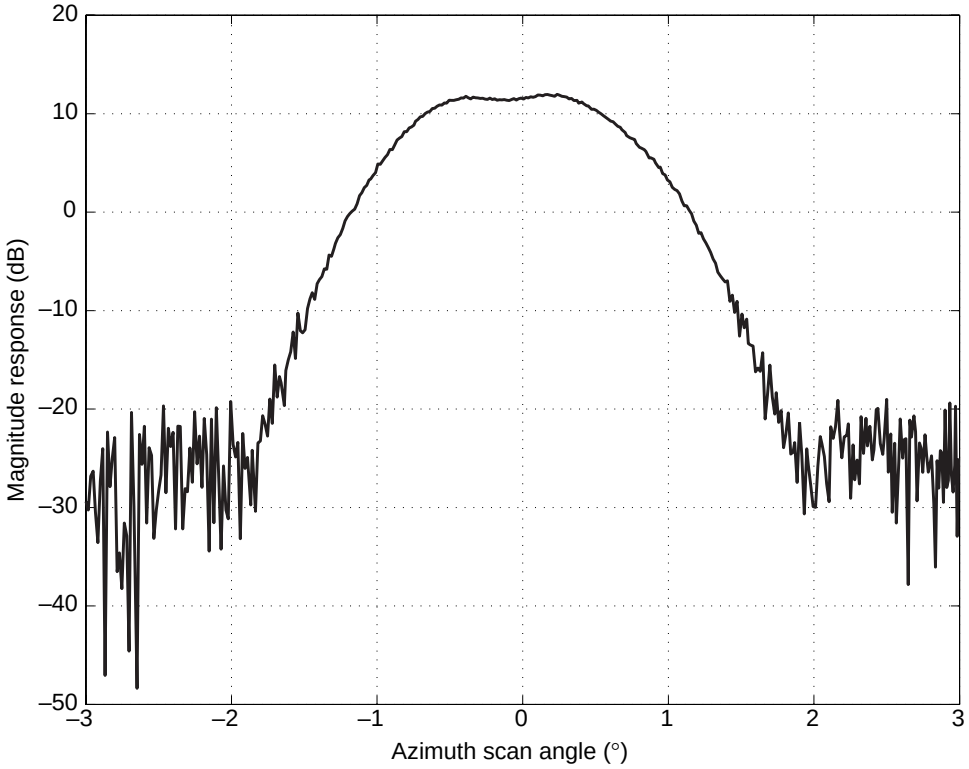

Figure A-9. LCERT data run 9 (SDP = 6).

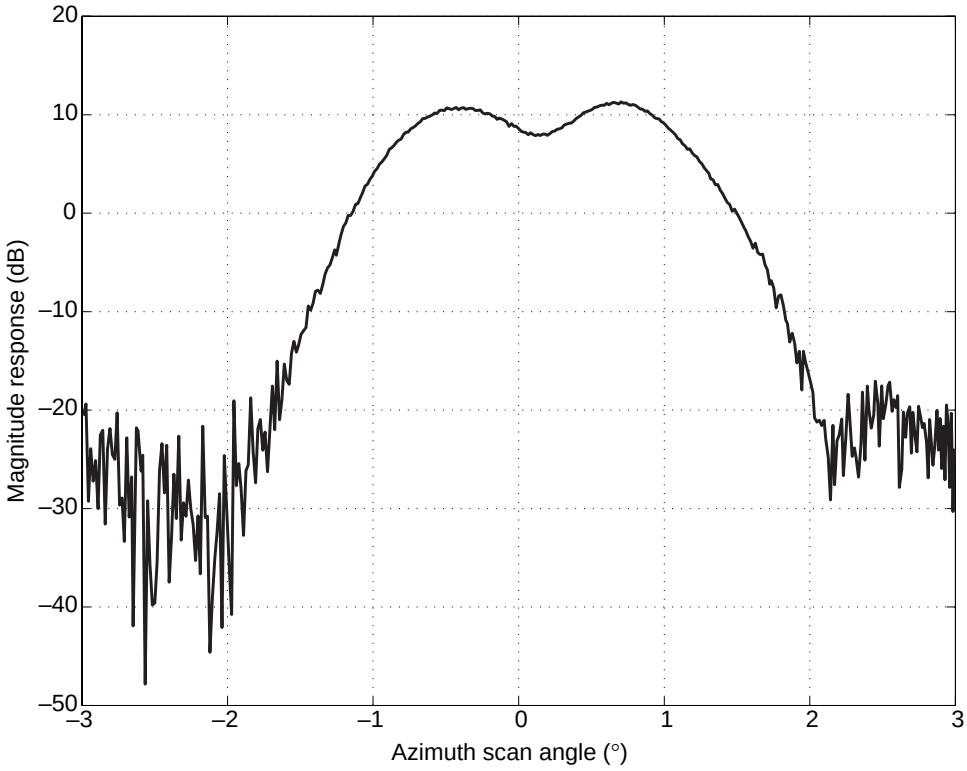

Figure A-10. LCERT data run 10 (SDP = 6).

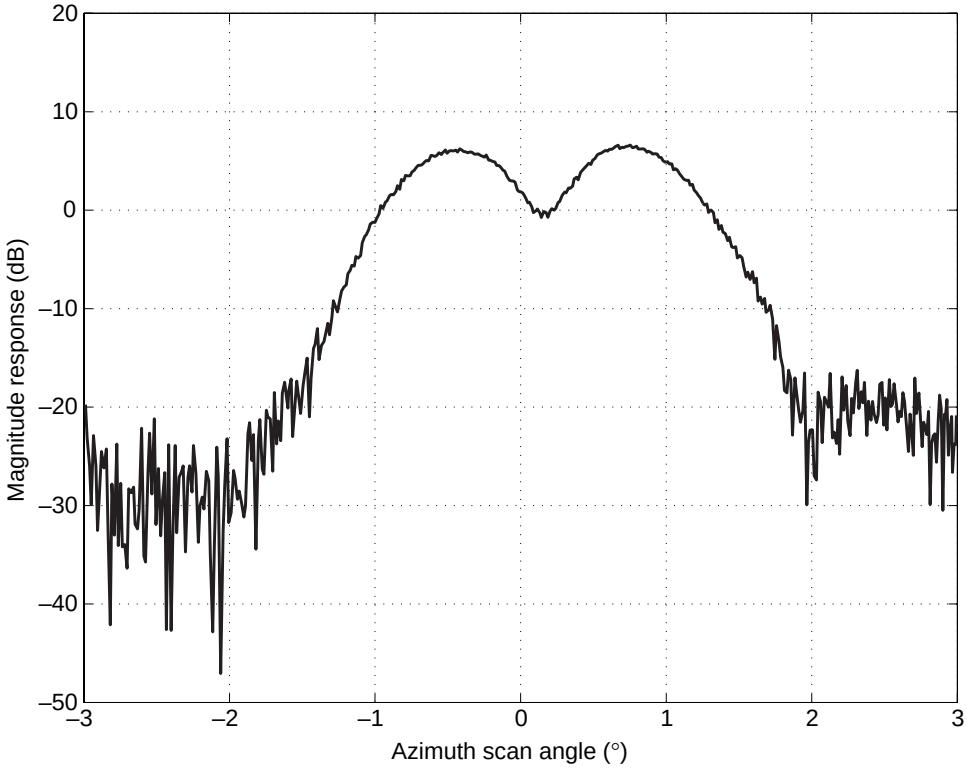

Figure A-11. LCERT data run 11 (SDP = 6).

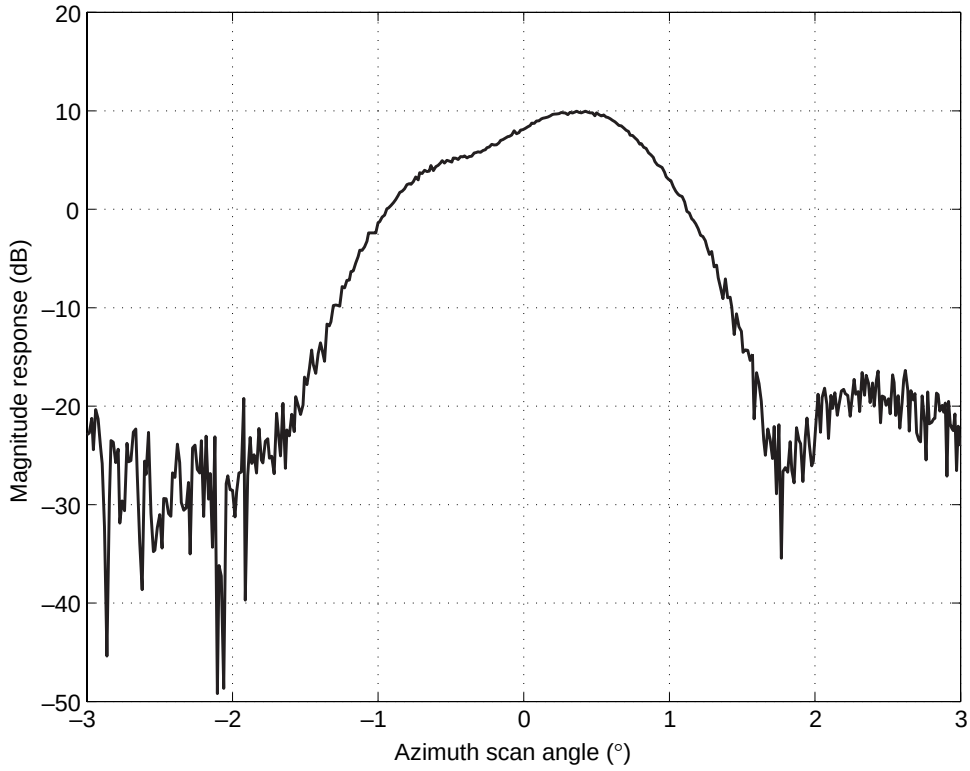

Figure A-12. LCERT data run 12 (SDP = 6).

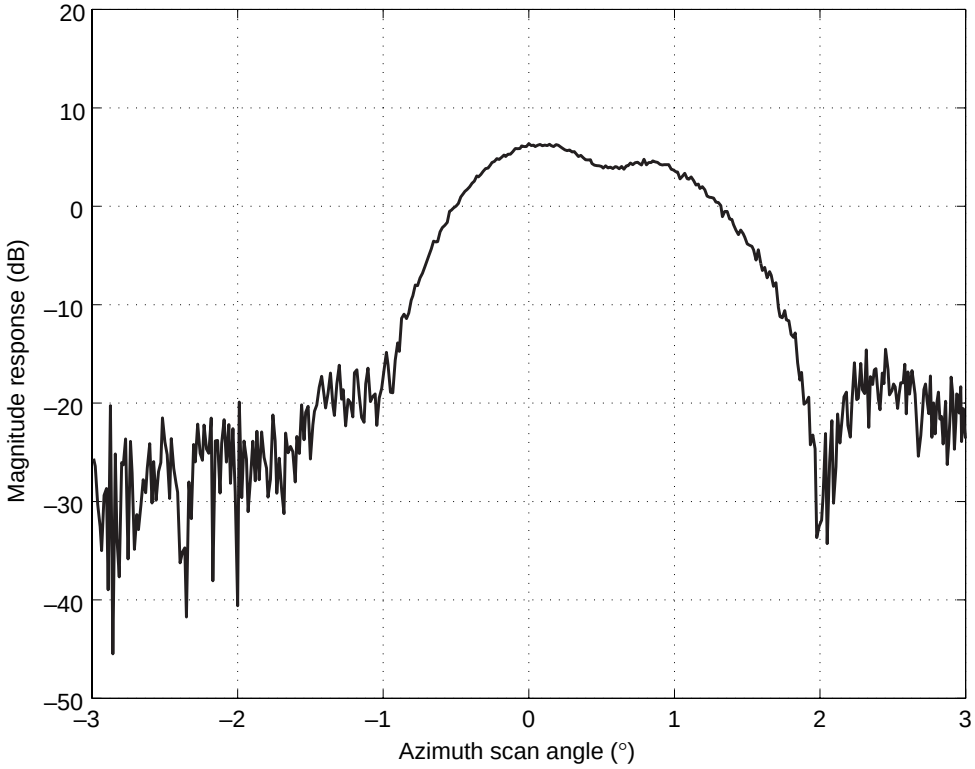

Figure A-13. LCERT data run 13 (SDP = 6).

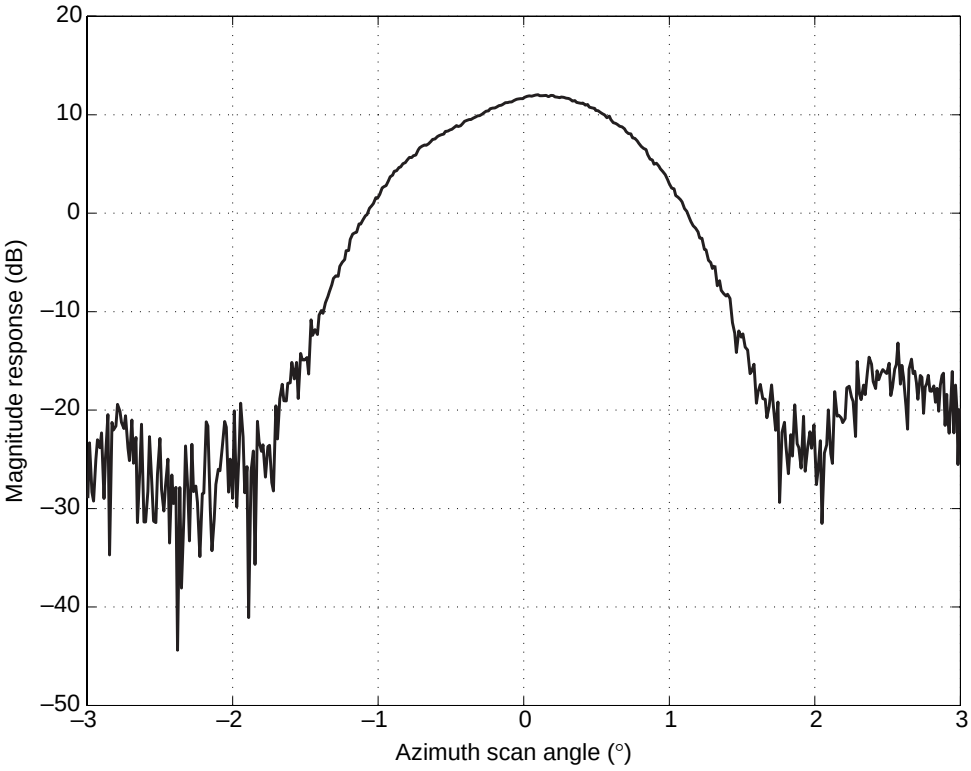

Appendix B. SMUSIC Outputs

Figure B-1. SMUSIC output for run 1 (skip data point (SDP) = 6, subvector averaging (SVA) = 4).

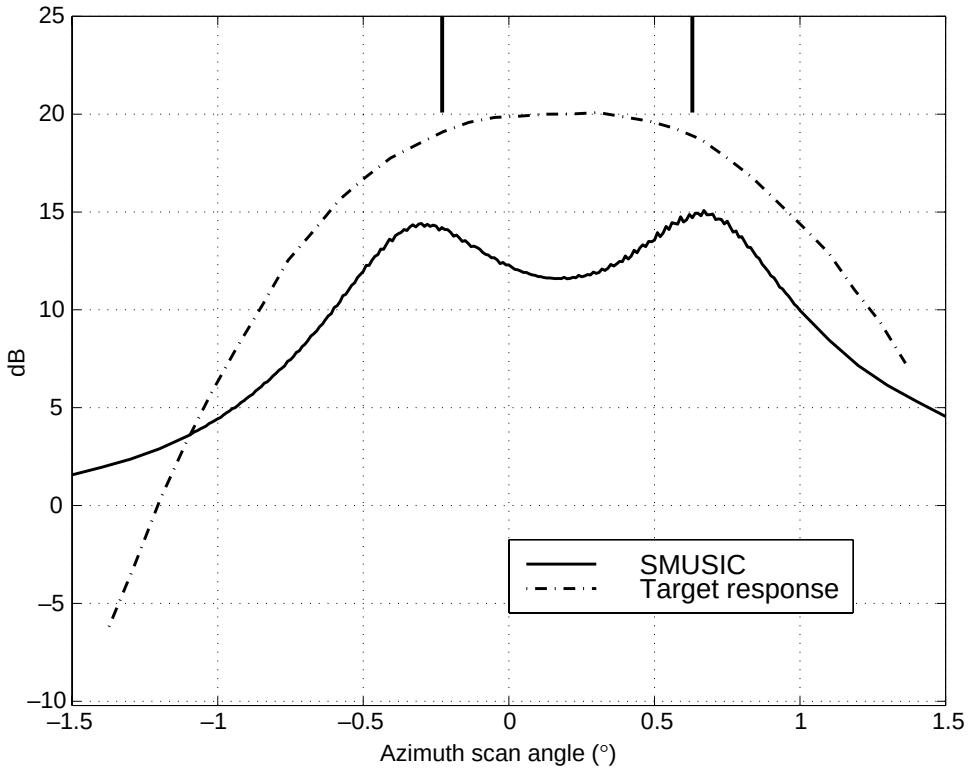

Figure B-2. SMUSIC output for run 2 (SDP = 6, SVA = 4).

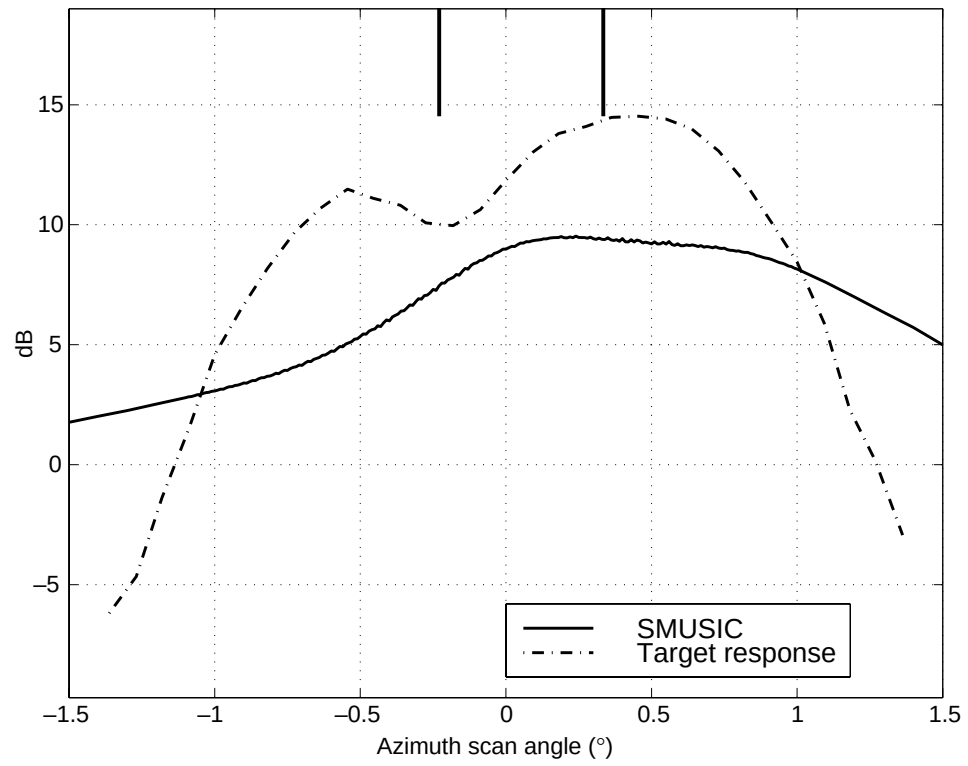

Figure B-3. SMUSIC output for run 4 (SDP = 6, SVA = 4).

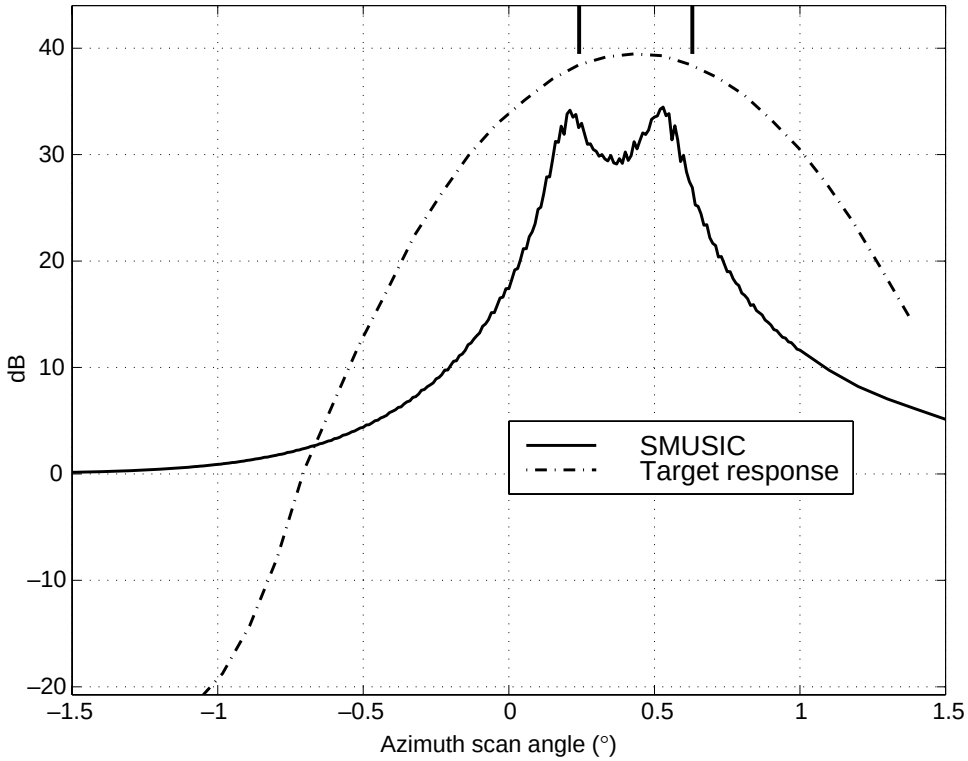

Figure B-4. SMUSIC output for run 5 (SDP = 6, SVA = 4).

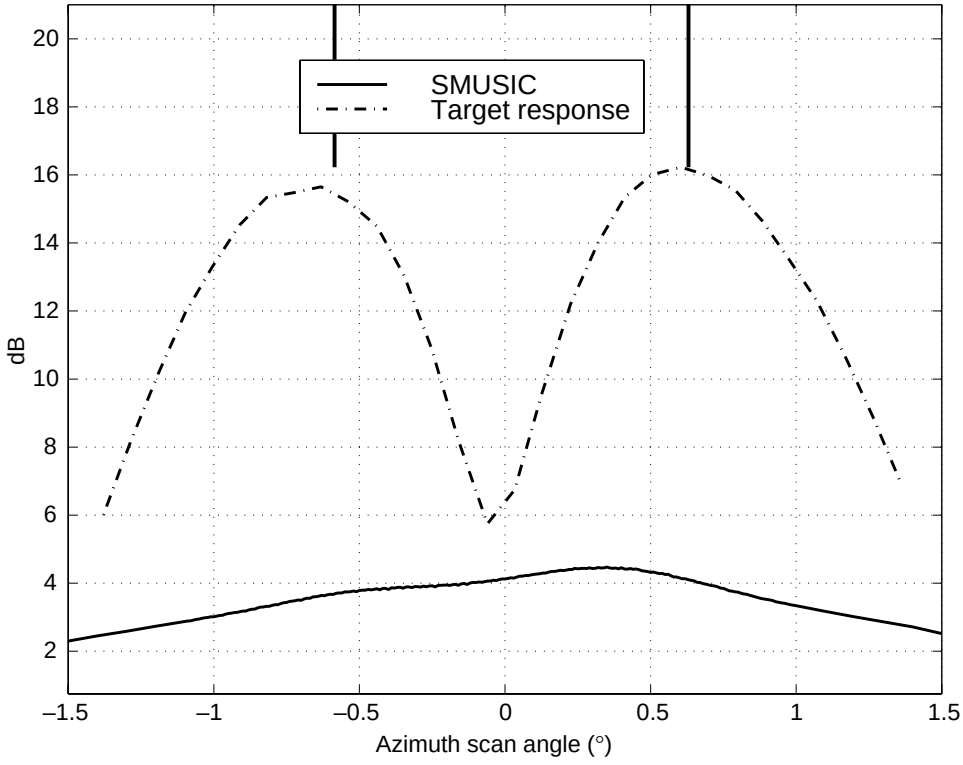

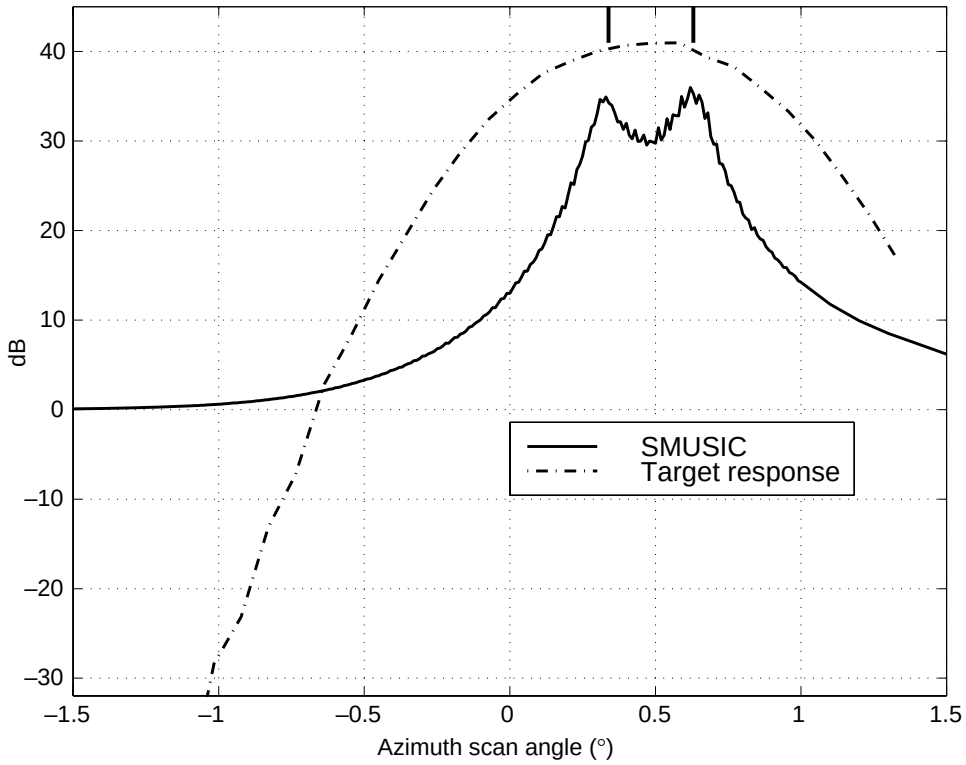

Figure B-5. SMUSIC output for run 6 (SDP = 6, SVA = 3).

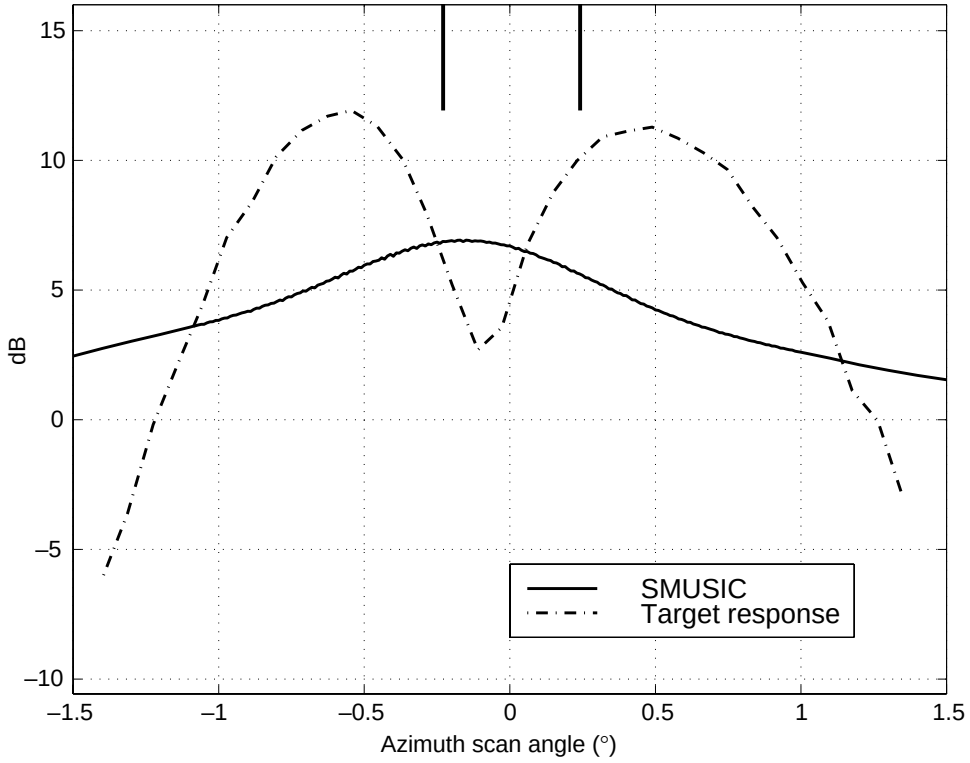

Figure B-6. SMUSIC output for run 7 (SDP = 6, SVA = 4).

Figure B-7. SMUSIC output for run 8 (SDP = 6, SVA = 4).

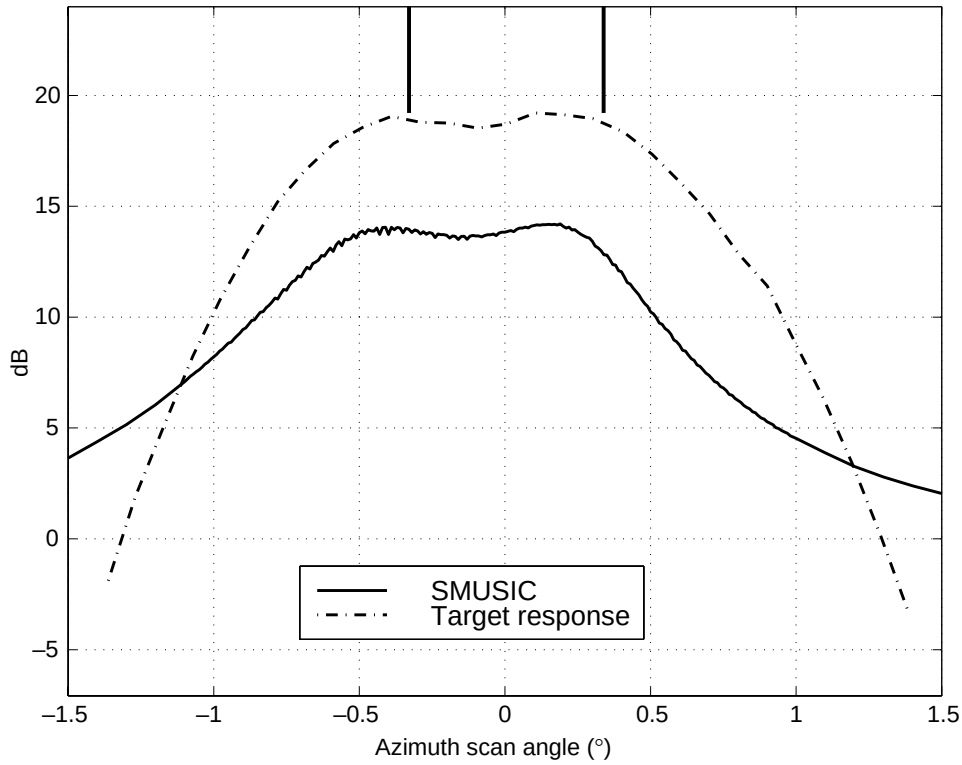

Figure B-8. SMUSIC output for run 9 (SDP = 6, SVA = 4).

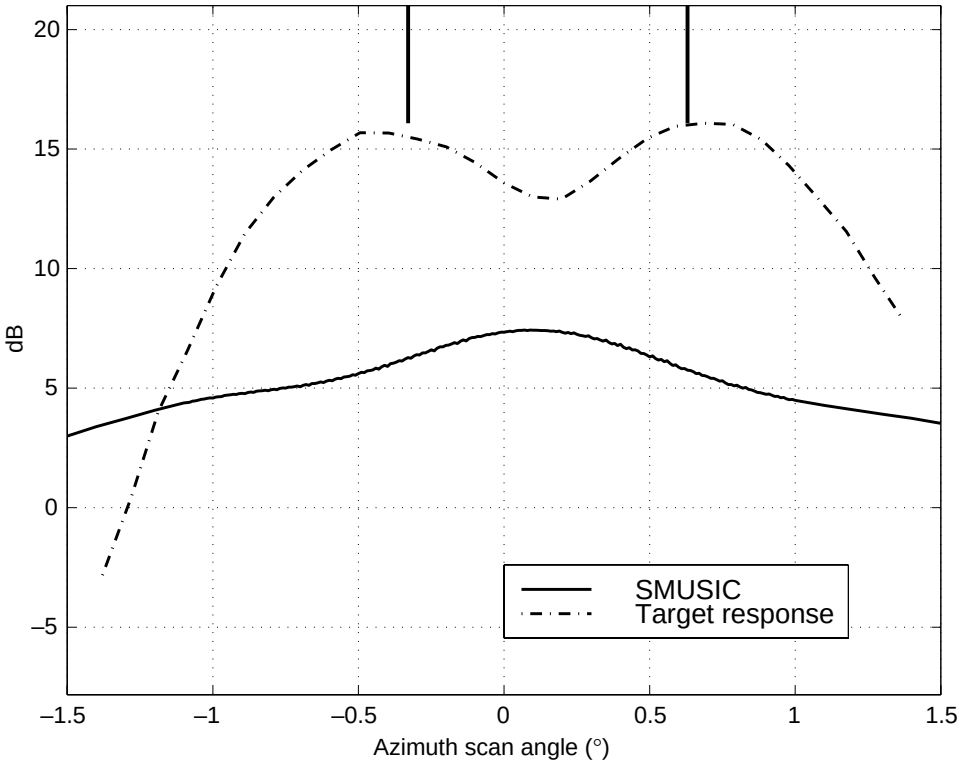

Figure B-9. SMUSIC output for run 10 (SDP = 6, SVA = 4).

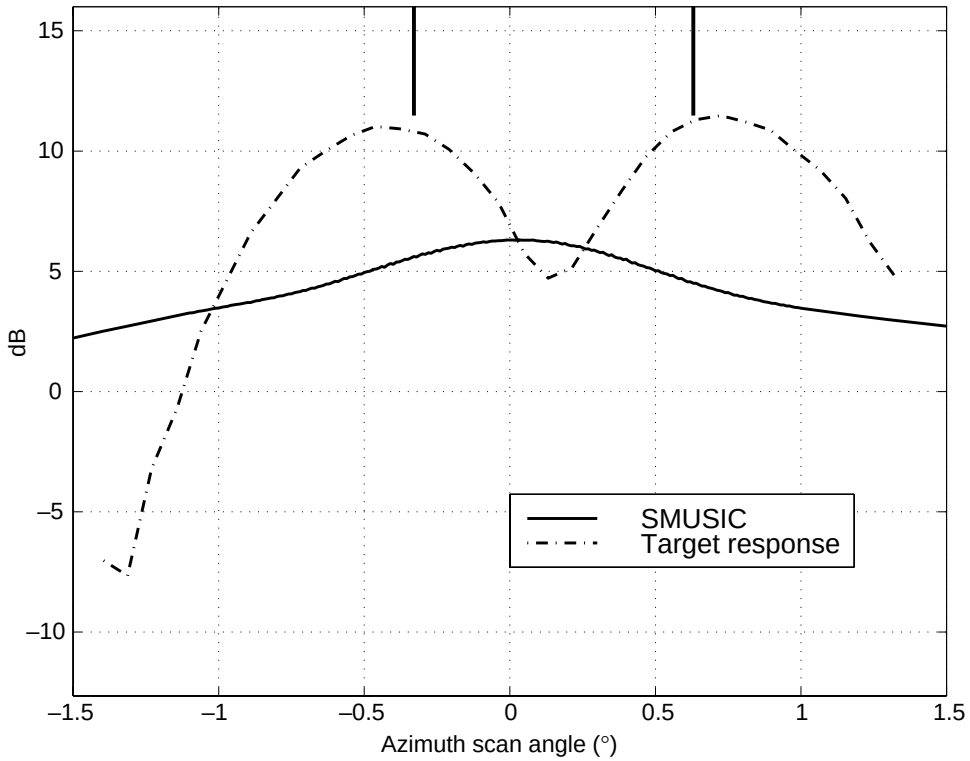

Figure B-10. SMUSIC output for run 11 (SDP = 6, SVA = 8).

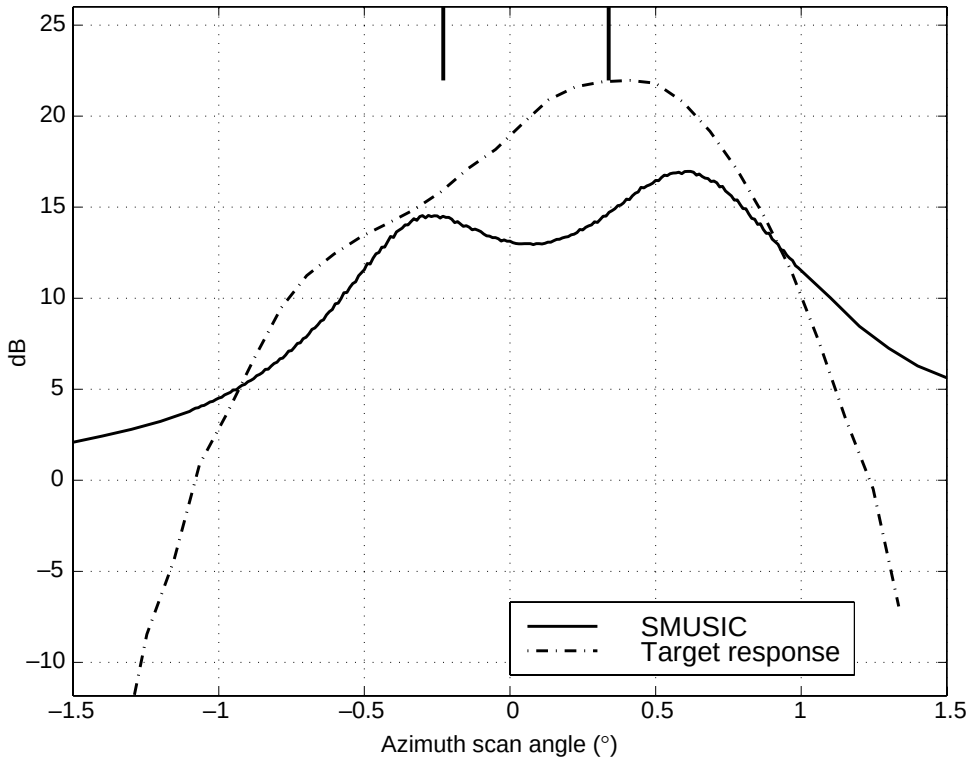

Figure B-11. SMUSIC output for run 12 (SDP = 6, SVA = 8).

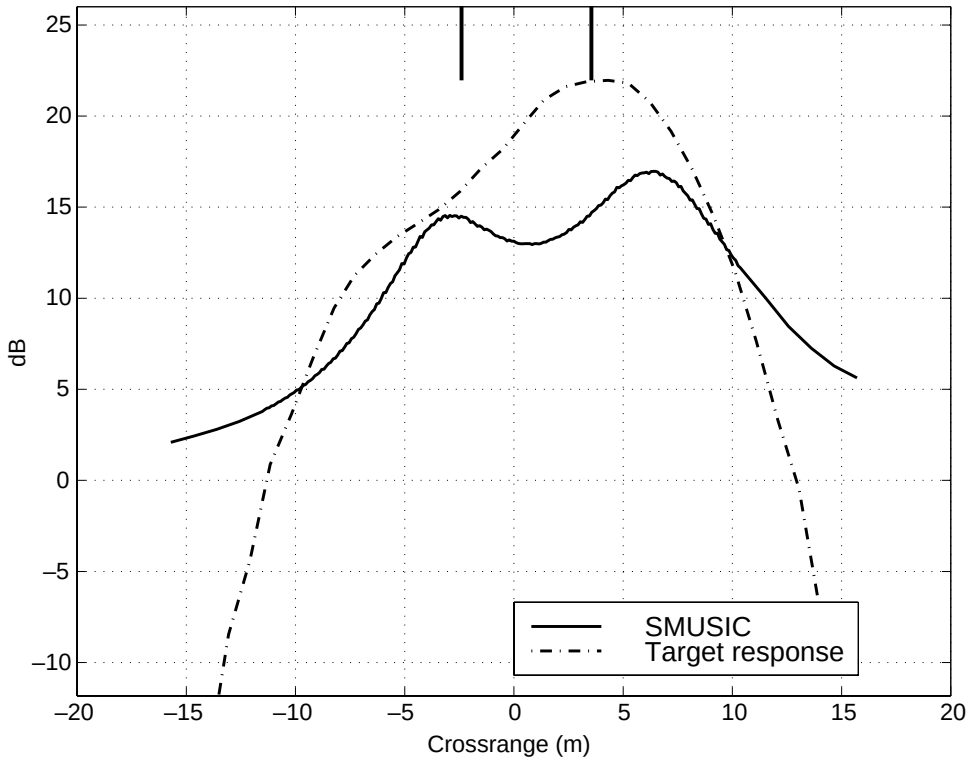

Figure B-12. SMUSIC output for run 13 (SDP = 6, SVA = 8).

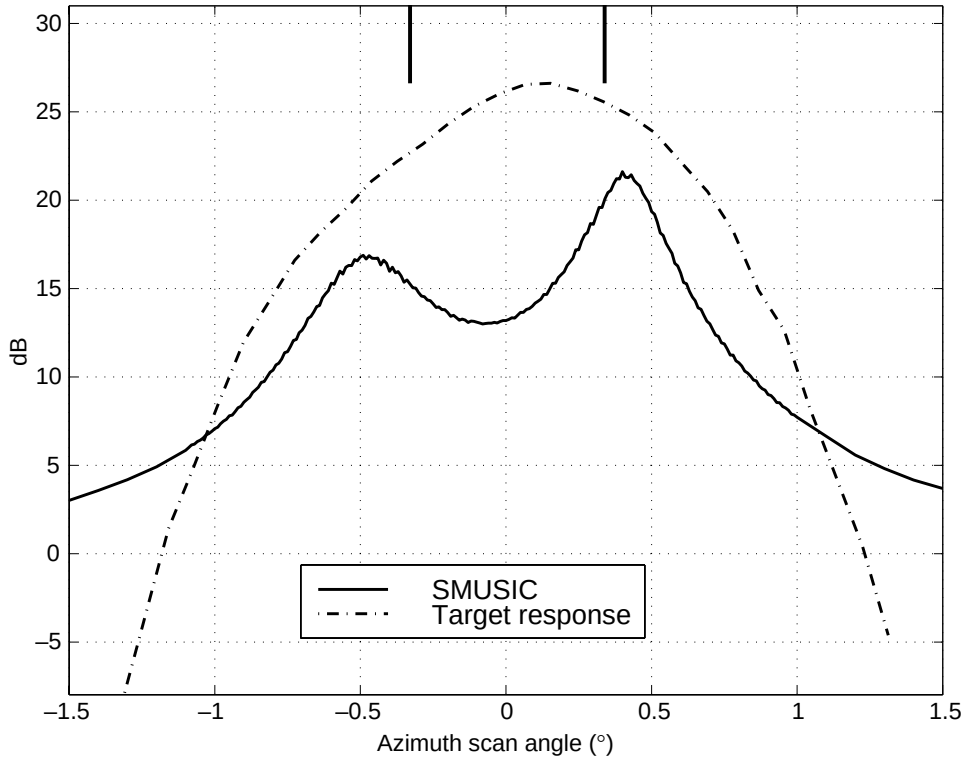

Distribution

Admnstr
Defns Techl Info Ctr
Attn DTIC-OCP
8725 John J Kingman Rd Ste 0944
FT Belvoir VA 22060-6218

Ofc of the Dir Rsrch and Engrg
Attn R Menz
Pentagon Rm 3E1089
Washington DC 20301-3080

Ofc of the Secy of Defns
Attn ODDRE (R&AT)
Attn ODDRE (R&AT) S Gontarek
The Pentagon
Washington DC 20301-3080

OSD
Attn OUSD(A&T)/ODDDR&E(R) R J Trew
Washington DC 20301-7100

AMCOM MRDEC
Attn AMSMI-RD W C McCorkle
Redstone Arsenal AL 35898-5240

CECOM
Attn PM GPS COL S Young
FT Monmouth NJ 07703

Dir for MANPRINT
Ofc of the Deputy Chief of Staff for Prsnnl
Attn J Hiller
The Pentagon Rm 2C733
Washington DC 20301-0300

Hdqtrs Dept of the Army
Attn DAMO-FDT D Schmidt
400 Army Pentagon Rm 3C514
Washington DC 20301-0460

US Army Edgewood RDEC
Attn SCBRD-TD J Vervier
Aberdeen Proving Ground MD 21010-5423

US Army Info Sys Engrg Cmnd
Attn ASQB-OTD F Jenia
FT Huachuca AZ 85613-5300

US Army Natick RDEC Acting Techl Dir
Attn SSCNC-T P Brandler
Natick MA 01760-5002

Director
US Army Rsrch Ofc
4300 S Miami Blvd
Research Triangle Park NC 27709

US Army Simulation, Train, & Instrmntn Cmnd
Attn J Stahl
12350 Research Parkway
Orlando FL 32826-3726

US Army Tank-Automtv & Armaments Cmnd
Attn AMSTA-AR-TD M Fisette
Bldg 1
Picatinny Arsenal NJ 07806-5000

US Army Tank-Automtv Cmnd Rsrch, Dev, & Engrg Ctr
Attn AMSTA-TA J Chapin
Warren MI 48397-5000

US Army Test & Eval Cmnd
Attn R G Pollard III
Aberdeen Proving Ground MD 21005-5055

US Army Train & Doctrine Cmnd
Battle Lab Integration & Techl Dirctrt
Attn ATCD-B J A Klevecz
FT Monroe VA 23651-5850

US Military Academy
Mathematical Sci Ctr for Excellence
Attn MDN-A MAJ M D Phillips
Dept of Mathematical Sci
West Point NY 10996

Nav Surface Warfare Ctr
Attn Code B07 J Pennella
17320 Dahlgren Rd Bldg 1470 Rm 1101
Dahlgren VA 22448-5100

DARPA
Attn B Kaspar
3701 N Fairfax Dr
Arlington VA 22203-1714

University of Texas ARL Electromag Group
Attn Campus Mail Code F0250 A Tucker
Austin TX 78713-8029

Distribution (cont'd)

Hicks & Associates, Inc
Attn G Singley III
1710 Goodrich Dr Ste 1300
McLean VA 22102

Palisades Inst for Rsrch Svc Inc
Attn E Carr
1745 Jefferson Davis Hwy Ste 500
Arlington VA 22202-3402

US Army Rsrch Lab
Attn AMSRL-CI-LL Techl Lib (3 copies)
Attn AMSRL-CS-AS Mail & Records Mgmt
Attn AMSRL-CS-EA-TP Techl Pub (3 copies)
Attn AMSRL-D J Lyons

US Army Rsrch Lab (cont'd)
Attn AMSRL-DD J Rocchio
Attn AMSRL-IS-CI J DeHart
Attn AMSRL-IS-TA B Sadler
Attn AMSRL-SE-R B Wallace
Attn AMSRL-SE-RM C Ly (10 copies)
Attn AMSRL-SE-RM E Burke
Attn AMSRL-SE-RM H Dropkin (10 copies)
Attn AMSRL-SE-RM J Nemarich
Attn AMSRL-SE-RM J Silverstein
Attn AMSRL-SE-RU J Costanza
Attn AMSRL-SE-SA T Pham
Attn AMSRL-SE-SR D Rodkey
Adelphi MD 20783-1197

REPORT DOCUMENTATION PAGE

Form Approved
OMB No. 0704-0188

1. AGENCY USE ONLY *(Leave blank)*	2. REPORT DATE	3. REPORT TYPE AND DATES COVERED
	October 1998	Final, Aug 97-Aug 98

4. TITLE AND SUBTITLE Superresolution for Low-Cost Enabling Radar Technology

5. FUNDING NUMBERS

DA PR: AH43
PE: 61102A

6. AUTHOR(S) Canh Ly and Herbert Dropkin

7. PERFORMING ORGANIZATION NAME(S) AND ADDRESS(ES)
U.S. Army Research Laboratory
Attn: AMSRL-SE-RL email: ly@arl.mil
2800 Powder Mill Road
Adelphi, MD 20783-1197

8. PERFORMING ORGANIZATION REPORT NUMBER
ARL-TR-1780

9. SPONSORING/MONITORING AGENCY NAME(S) AND ADDRESS(ES)
U.S. Army Research Laboratory
2800 Powder Mill Road
Adelphi, MD 20783-1197

10. SPONSORING/MONITORING AGENCY REPORT NUMBER

11. SUPPLEMENTARY NOTES
ARL PR: 8NE2HH
AMS code: 611102.H43

12a. DISTRIBUTION/AVAILABILITY STATEMENT Approved for public release; distribution unlimited.

12b. DISTRIBUTION CODE

13. ABSTRACT *(Maximum 200 words)*

The MUltiple SIgnal Classification (MUSIC) algorithm has been used widely in applications with spatially distributed sensor arrays. In these applications, the algorithm uses the phase relations of the signal at different sensor pointing angles. Accordingly, the MUSIC algorithm has not been used by others to superresolve target positions within the main beam of a radar with a single narrow-beam antenna that is step-scanned in angle because there is no phase shift due to the scanning of the beam. We have developed an application called Scan MUSIC (SMUSIC) for the spatial resolution of closely spaced targets with a stepped-scan radar. We apply SMUSIC to resolve closely spaced coherent targets when a one-dimensional stepped scanning antenna is used. As the low-cost enabling radar technology (LCERT) antenna points at different angles in the horizontal (azimuth) direction, a step-scan sensor vector is formed. In this report, we demonstrate that SMUSIC can be used for a scanning antenna using experimental LCERT radar data. We also show the problems encountered when using experimental data from targets exhibiting constructive and destructive interferences.

14. SUBJECT TERMS
superresolution, MUSIC, Scan MUSIC, scanning antenna, LCERT, forward subvector averaging

15. NUMBER OF PAGES
37

16. PRICE CODE

17. SECURITY CLASSIFICATION OF REPORT	18. SECURITY CLASSIFICATION OF THIS PAGE	19. SECURITY CLASSIFICATION OF ABSTRACT	20. LIMITATION OF ABSTRACT
Unclassified	Unclassified	Unclassified	UL

NSN 7540-01-280-5500

Standard Form 298 (Rev. 2-89)
Prescribed by ANSI Std. Z39-18
298-102

DEPARTMENT OF THE ARMY
U.S. Army Research Laboratory
2800 Powder Mill Road
Adelphi, MD 20783-1197